



Cite this: *Chem. Commun.*, 2015, 51, 14469

Received 10th June 2015,  
Accepted 3rd August 2015

DOI: 10.1039/c5cc04803f

www.rsc.org/chemcomm

# Mechanistic elucidation of C–H oxidation by electron rich non-heme iron(IV)–oxo at room temperature†

Sujoy Rana, Aniruddha Dey and Debabrata Maiti\*

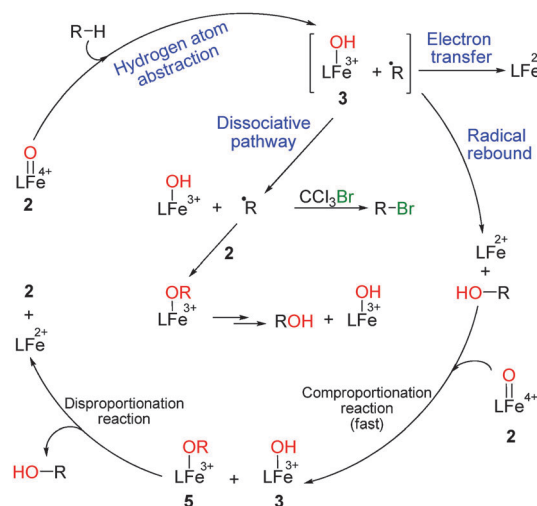
**Non-heme iron(IV)–oxo species form iron(III) intermediates during hydrogen atom abstraction (HAA) from the C–H bond. While synthesizing a room temperature stable, electron rich, non-heme iron(IV)–oxo compound, we obtained iron(III)–hydroxide, iron(III)–alkoxide and hydroxylated-substrate-bound iron(II) as the detectable intermediates. The present study revealed that a radical rebound pathway was operative for benzylic C–H oxidation of ethylbenzene and cumene. A dissociative pathway for cyclohexane oxidation was established based on UV-vis and radical trap experiments. Interestingly, experimental evidence including O-18 labeling and mechanistic study suggested an electron transfer mechanism to be operative during C–H oxidation of alcohols (e.g. benzyl alcohol and cyclobutanol). The present report, therefore, unveils non-heme iron(IV)–oxo promoted substrate-dependent C–H oxidation pathways which are of synthetic as well as biological significance.**

High-valent iron–oxo species are responsible for C–H oxidations in numerous biological and chemical transformations for both heme and non-heme enzymes.<sup>1</sup> Heme enzymes like cytochrome P450 carry out alkane hydroxylation, olefin epoxidation and sulfoxidation involving the iron(IV)–oxo porphyrin  $\pi$ -cation radical.<sup>2</sup> Non-heme enzymes, such as Rieske oxygenase, and  $\alpha$ -ketoglutarate dependent dioxygenases, TauD-J, routinely perform biochemical oxidative transformations involving the iron(IV)–oxo intermediate. Intense experimental work has been devoted for mimicking the chemistry of heme/non-heme enzymes.<sup>3</sup>

Non-heme iron(IV)–oxo complexes abstract hydrogen atoms from C–H bonds in the rate determining step to form iron(III) hydroxide and radical species ( $R^\bullet$ ).<sup>4</sup> These active species, depending on their properties, can pursue a radical rebound, radical non-rebound or electron transfer mechanism to form the respective C–H oxidation products (Scheme 1).<sup>4,5</sup> Following a radical rebound pathway, the *in situ* formed iron(II)–species

and alcohol can undergo the comproportionation reaction in the presence of another equivalent of iron(IV)–oxo (Scheme 1).<sup>3b</sup> In the case of a dissociative pathway, iron(III)–hydroxide and the substrate radical (generated upon HAA) become separated from the solvent cage resulting in subsequent radical trapped products and other side reactions of iron(III)–hydroxides. Such a pathway is well accepted for the iron(IV)–oxo and manganese(IV)–oxo complexes.<sup>5,6</sup>

Although the radical rebound pathway has been established for ruthenium(IV)–oxo,<sup>7</sup> gathering concrete evidence for the same in the case of iron(IV)–oxo requires further study. We thought of synthesizing a modified N4Py ligand scaffold (L) with electron rich substituents at the picolyl moiety. We were particularly intrigued by the DFT data of Fe–(N4Py) complex which showed greater HOMO contribution by two picolyl moieties that resulted in a shorter Fe–N(picolyl) distance in the Fe–(N4Py) complex.<sup>8</sup> We rationalized that the introduction of an electron donating group (such as 4-OMe) in the picolyl unit would further shorten the Fe–(N4Py) distance and would



Scheme 1 C–H oxidations by non-heme iron(IV)–oxo.

Department of Chemistry, Indian Institute of Technology Bombay, Powai, Mumbai 400076, India

† Electronic supplementary information (ESI) available. CCDC 1051845. For ESI and crystallographic data in CIF or other electronic format see DOI: 10.1039/c5cc04803f



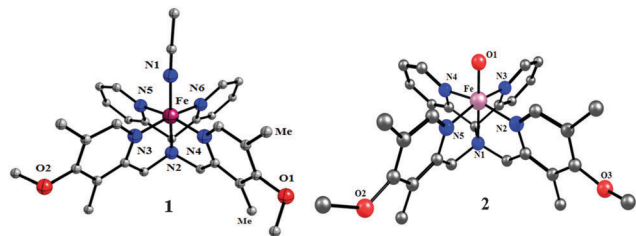
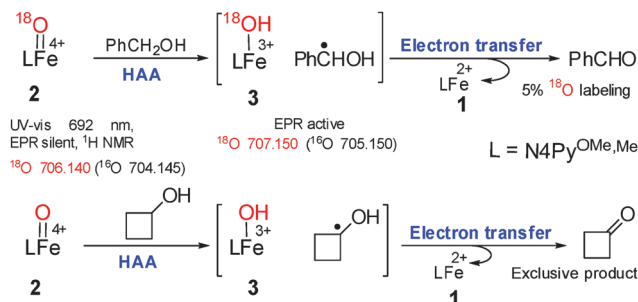


Fig. 1 ORTEP diagram of complex **1** (CCDC 1051845) and DFT optimized geometry of **2** using B3LYP/LANL2DZ with N4Py<sup>OMe,Me</sup> ligand.

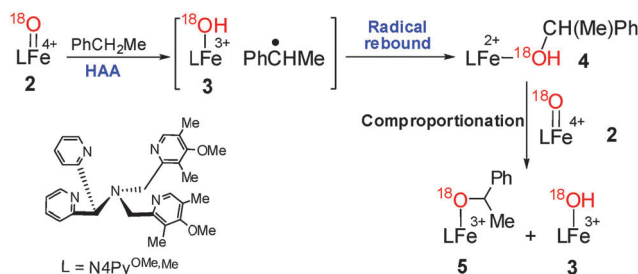
increase the HOMO contribution (Fig. 1).<sup>8</sup> Consequently, it would produce more reactive reaction intermediates, which could be verified by detailed mechanistic studies.<sup>3d-f,4a,b</sup>

The non-heme iron complex  $[(\text{N4Py})^{\text{OMe,Me}}\text{Fe}^{\text{II}}(\text{CH}_3\text{CN})](\text{OTf})_2$  (**1**) was synthesized by reacting  $\text{Fe}(\text{OTf})_2 \cdot 2\text{CH}_3\text{CN}$  with an electronically enriched and substituted N4Py<sup>OMe,Me</sup> ligand.<sup>5</sup> Complex **1** was also characterized using X-ray spectroscopy (Fig. 1), ESI-MS ( $m/z$ , 688.150), UV-vis spectroscopy (maximum at 459 nm due to LMCT),<sup>9</sup> NMR (0–10 ppm, <sup>1</sup>H- and 0–200 ppm, <sup>13</sup>C-) and EPR (silent) studies indicated the diamagnetic character of **1**.<sup>10,11</sup> Electrochemical studies of complex **1** showed a lower  $\text{Fe}^{\text{III}}/\text{Fe}^{\text{II}}$  reduction potential ( $E_{1/2} \sim 0.84$  V vs. SCE) compared to that of the unsubstituted N4Py iron(II) complex ( $E_{1/2} \sim 1.01$  V vs. SCE).<sup>8,12</sup> This further suggested that iron(III) species for **1** is more stable compared to that of the unsubstituted N4Py iron(III) complex. The corresponding iron(IV)-oxo species,  $[(\text{N4Py})^{\text{OMe,Me}}\text{Fe}^{\text{IV}}(\text{O})]^{2+}$  (**2**) was synthesized by reacting **1** with iodosyl benzene in acetonitrile at room temperature. A characteristic UV-vis maximum at 692 nm ( $\epsilon \sim 432 \text{ M}^{-1} \text{ cm}^{-1}$ ) due to ligand field transitions (d–d transition) was also observed.<sup>4a,13</sup> Complex **2** showed a slightly more negative  $\text{Fe}^{\text{IV}}/\text{Fe}^{\text{III}}$  reduction potential ( $E_{\text{p,c}} \sim -0.19$  V vs. SCE) compared to the unsubstituted  $[(\text{N4Py})\text{Fe}^{\text{IV}}(\text{O})]^{2+}$  ( $E_{\text{p,c}} \sim -0.15$  V vs. SCE). Notably, **2** was found to be stable at room temperature for a few days ( $t_{1/2} \sim 50$  h at 30 °C in air).<sup>8</sup> The ESI-MS characterization of complex **2** revealed a major isotopic peak at 704.145 due to  $[(\text{N4Py})^{\text{OMe,Me}}\text{Fe}^{\text{IV}}(\text{O})](\text{OTf})^+$  which was shifted to 706.150 upon O-18 labeling with  $\text{H}_2^{18}\text{O}$  ( $\sim 95\%$  O-18 incorporation, *vide infra*).<sup>14</sup> The <sup>1</sup>H NMR spectrum (–20 to 50 ppm) along with the EPR silent behaviour at 77 K suggested a paramagnetic character of **2** (likely in the  $S = 1$  spin state).<sup>10,15</sup>

Oxidation of benzyl alcohol by **2** provided benzaldehyde as the sole product (yield, 86%). Labeling studies showed 5% O-18 incorporation into benzaldehyde. Furthermore, C–H oxidation of  $\text{PhCH}_2\text{OH}$  and  $\text{PhCD}_2\text{OH}$  ( $\sim 95\%$ , D enriched) provided a kinetic isotope effect value of 11 which suggests that the initial hydrogen atom abstraction is the rate determining step.<sup>3b,8,16</sup> Cyclobutanol as the mechanistic probe provided cyclobutanone exclusively ( $2e^-$  oxidation product) (the ring opening product 4-hydroxybutanal was not detected) without any O-18 labeling (Scheme 2). These observations suggest that following HAA, an electron transfer mechanism is operational during C–H oxidation of benzyl alcohol.<sup>16,17</sup> Subsequently, we studied the C–H oxidation chemistry of **2** using ethylbenzene (Scheme 3), cumene and cyclohexane.<sup>8</sup> Cyclohexane produced cyclohexanol ( $\sim 15\%$  yield, 52% O-18 enriched) whereas ethyl benzene gave 1-phenyl ethanol (yield, 22%; 60% O-18 labeled).



Scheme 2 Alcohol oxidations by  $[(\text{N4Py})^{\text{OMe,Me}}\text{Fe}^{\text{IV}}(\text{O})]^{2+}$  (**2**).



Scheme 3 Intermediates during reaction of **2** and ethylbenzene.

The ESI-MS data obtained upon addition of ethylbenzene to **2** suggested the formation of iron(III)-hydroxide (**3**,  $m/z$ , 705.150), 1-phenylethanol bound intermediate,  $[(\text{N4Py})^{\text{OMe,Me}}\text{Fe}^{\text{II}}(\text{HO}(\text{Me})\text{CHPh})](\text{OTf})^+$  (**4**,  $m/z$ , 810.22; Fig. 2g) and iron(III)-alkoxide,  $[(\text{N4Py})^{\text{OMe,Me}}\text{Fe}^{\text{III}}(\text{O}(\text{Me})\text{CHPh})](\text{OTf})^+$  (**5**,  $m/z$ , 809.215; Fig. 2b and e) (Scheme 3). Most interestingly, the 1-phenylethanol bound intermediate  $[(\text{N4Py})^{\text{OMe,Me}}\text{Fe}^{\text{II}}(\text{HO}(\text{Me})\text{CHPh})](\text{OTf})^+$  (**4**) formed as a consequence of the radical rebound step was rapidly oxidized by **2** to produce **3** and **5**.<sup>7</sup> The formation of **5** occurred *via* the comproportionation reaction of **1** and **2** in the presence of 1-phenyl ethanol. This was further verified by adding 1-phenyl ethanol to a solution of **2** in acetonitrile where both **3** and **5** were simultaneously detected.

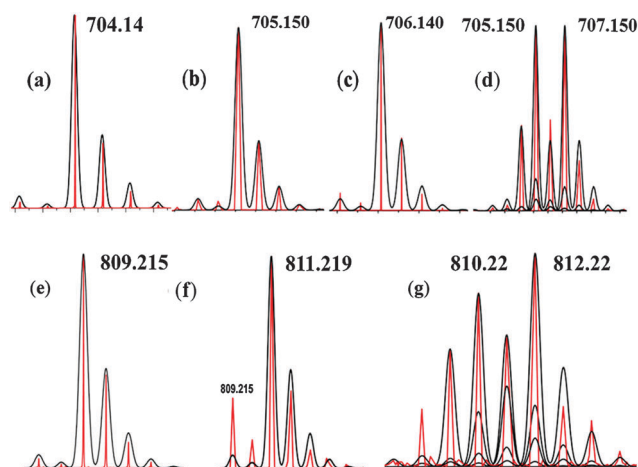


Fig. 2 ESI-MS of the intermediates during reaction of **2** and ethylbenzene (red line, experimental and black line, simulated, spectra were recorded after 5 min of addition). ESI-MS of **2** (a), **3** (b), 18-O-**2** (c), 18-O-**3** (d), **5** (e), 18-O-**5** (f), **4** and 18-O-**4** (g).<sup>8</sup>



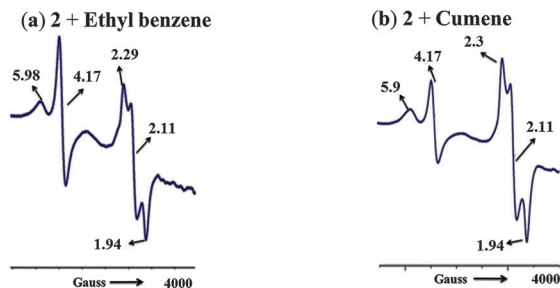


Fig. 3 EPR spectra (acetonitrile, 77 K) obtained from reaction between **2** and (a) ethylbenzene (b) cumene.

Furthermore, the formation of iron(III) complex was confirmed from rhombic signals at  $g_1 = 1.94$ ,  $g_2 = 2.11$ ,  $g_3 = 2.10$  and axial signals at  $g_1 = 4.17$ ,  $g_2 = 5.98$  by the EPR experiment of a solution of **2** and ethyl benzene (or cumene) (Fig. 3a and b).<sup>5,15,18</sup> Replacing ethyl benzene by cumene also showed the formation of iron(III)-hydroxide (**3**) and iron(III)-alkoxide species,  $[(\text{N4Py})^{\text{OMe,Me}}\text{Fe}^{\text{III}}(\text{O}(\text{Me})_2\text{CPh})](\text{OTf})^+$  (**5a**,  $m/z$ , 823.21; Scheme 4), which upon  $^{18}\text{O}$  labeling shifted by two mass units ( $m/z$ , 825.21; Fig. 4a and b) along with 70% O-18 enriched cumyl alcohol.

The formation of **5a** was presumed to occur *via* the comproportionation reaction. This was verified when 2-phenyl-2-propanol was added to a solution of **2**; trace amounts of **3** and **5a** were observed after 30 min. Notably, a significant amount of these compounds was formed after 16 h. Complex **2** decayed with time to form **1**, which in the presence of 2-phenyl-2-propanol and **2** underwent the comproportionation reaction to form **3** and **5a**. Expectedly, formation of **3** and **5a** (Scheme 4) was observed within 10 minutes *via* the comproportionation reaction when 2-phenyl-2-propanol was added to a mixture of **1** and **2**.

In the presence of ethylbenzene (or cumene), the absorbance *vs.* time plot for complex **2** (decay profile at 692 nm) was fitted

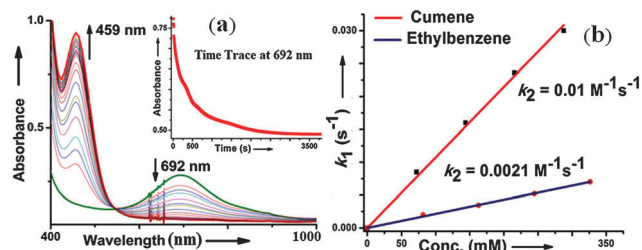


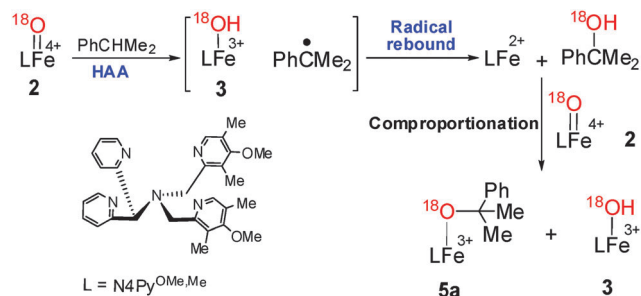
Fig. 5 (a) UV-vis change at 692 nm for **2**, in presence of cumene, (b) kinetics plot for cumene and ethylbenzene.

with the pseudo-first order reaction profile (rate constant,  $k_1$ ; Fig. 5).<sup>3b,4a,5</sup> A straight line was obtained by plotting the different values of  $k_1$  against concentration of the substrate. The slope of this plot yielded the second order rate constant ( $k_2$ , Fig. 5).<sup>8</sup> During the C–H oxidation reaction by **2**, cumene reacted slightly faster ( $k_2 \sim 0.01 \text{ M}^{-1} \text{ s}^{-1}$ ) compared to ethylbenzene ( $k_2 \sim 0.0021 \text{ M}^{-1} \text{ s}^{-1}$ ) due to the higher strength of the benzylic C–H bond.<sup>19</sup> The reaction of cumene with complex **2** occurred at a slightly faster rate ( $\sim 5$  times,  $k_2 \sim 0.01 \text{ M}^{-1} \text{ s}^{-1}$  *vs.*  $k_2 = 0.002 \text{ M}^{-1} \text{ s}^{-1}$  for  $\text{Fe-N4Py-oxo}$ )<sup>4a</sup> compared to that for the unsubstituted  $\text{Fe-N4Py-oxo}$  complex. However, the reaction rate of **2** with ethylbenzene is similar to that of its unsubstituted analogue ( $0.0021 \text{ M}^{-1} \text{ s}^{-1}$  *vs.*  $0.0031 \text{ M}^{-1} \text{ s}^{-1}$  or  $0.008 \text{ M}^{-1} \text{ s}^{-1}$ ).<sup>4a,5</sup> Notably, during the C–H oxidation reactions of **2** with ethylbenzene, cumene, triphenyl methane, benzyl alcohol and cyclobutanol (500 equiv.) iron(II) were regenerated. Initially, after 1–2 hours of the reaction, 40–60% of iron(II) species was regenerated. After 48 hours of the reaction, iron(II) was obtained quantitatively ( $\sim 95\%$ ). On the contrary, the unsubstituted  $[\text{Fe}^{\text{II}}(\text{N4Py})(\text{O})]^{2+}$  complex generated  $\sim 95\%$  of the iron(III) species *via* a dissociative pathway after completion of the reaction with ethyl benzene, cumene and triphenyl methane.<sup>5</sup>

Cyclohexane oxidation by **2** produced a major amount of iron(III) ( $\sim 90\%$ ) and minor amount of iron(II) species (10%). Moreover, the cyclohexyl radical was trapped in the form of cyclohexyl bromide upon addition of  $\text{CCl}_3\text{Br}$  (or  $\text{CBr}_4$ ) during cyclohexane oxidation by **2**.<sup>8,11</sup> These experimental pieces of evidence suggested that cyclohexane oxidation was likely following a dissociative pathway.

No radical trapped or brominated product was found during the reaction of **2** with ethylbenzene or cumene.<sup>11,20</sup> Therefore, the substrate based organic radicals failed to escape from the solvent cage for ethylbenzene and cumene.<sup>20c</sup> Although radicals formed *via* the dissociative pathway have been trapped as per the prescient knowledge reported in the literature for non-heme iron(IV)-oxo, our experimental observations suggested that following HAA, the iron(III)-hydroxide and the exogenous substrate based radical may not undergo dissociation (*e.g.* in the case of ethylbenzene and cumene).<sup>21</sup> The reaction followed a radical rebound pathway and produced an iron(II)-alcohol coordinated product that was subsequently oxidized by **2**.<sup>20c</sup>

In summary, we have synthesized an electron rich, room temperature stable and reactive non-heme iron(IV)-oxo species  $[(\text{N4Py})^{\text{OMe,Me}}\text{Fe}^{\text{IV}}(\text{O})](\text{OTf})^+$  (**2**). The iron(IV)-oxo derived intermediates like iron(III)-hydroxide (**3**), iron(III)-alkoxide (**5**) and substrate-bound



Scheme 4 Radical rebound pathway for C–H oxidation of cumene.

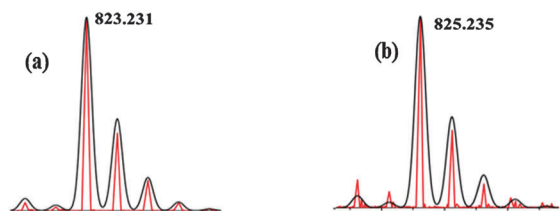


Fig. 4 ESI-MS of the intermediates, **5a** (a) and  $^{18}\text{O}$ -labeled **5a** (b) during reaction of **2** and cumene (red line, experimental and black line, simulated).





iron(II) species (**4**) were detected from the reaction mixture. The mechanistic switch during C–H oxidation by non-heme iron(IV)–oxo complex **2** mainly depends on the stability of the radical generated after HAA. More stable radicals preferred the electron transfer pathway (Scheme 2), whereas moderately stable radicals underwent the radical rebound pathway (Schemes 3 and 4). The least stable radicals of all (e.g. in case of cyclohexane) underwent the dissociative pathway.

This study was supported by SERB, India (EMR/2015/000164). Financial support received from CSIR-India (fellowships to S. R.) is gratefully acknowledged. DM sincerely thanks Dr. Sayam Sen Gupta (NCL Pune), Dr. Tapan K. Paine (IACS Kolkata) and their group members for stimulating scientific discussions and providing constant support to conduct a number of experiments in their laboratories.

## Notes and references

- (a) L. Que, Jr. and W. B. Tolman, *Nature*, 2008, **455**, 333; (b) M. Costas, M. P. Mehn, M. P. Jensen and L. Que Jr., *Chem. Rev.*, 2004, **104**, 939; (c) K. Ray, F. F. Pfaff, B. Wang and W. Nam, *J. Am. Chem. Soc.*, 2014, **136**, 13942; (d) B. Meunier, S. P. de Visser and S. Shaik, *Chem. Rev.*, 2004, **104**, 3947; (e) J. Rittle and M. T. Green, *Science*, 2010, **330**, 933; (f) C. Krebs, D. Galonić Fujimori, C. T. Walsh and J. M. Bollinger, *Acc. Chem. Res.*, 2007, **40**, 484; (g) S. Fukuzumi, *Coord. Chem. Rev.*, 2013, **257**, 1564; (h) O. Y. Lyakin and A. A. Shteinman, *Kinet. Catal.*, 2012, **53**, 694; (i) E. I. Solomon, S. D. Wong, L. V. Liu, A. Decker and M. S. Chow, *Curr. Opin. Chem. Biol.*, 2009, **13**, 99; (j) X. Shan and L. Que, Jr., *J. Inorg. Biochem.*, 2006, **100**, 421; (k) A. R. McDonald and L. Que Jr., *Coord. Chem. Rev.*, 2013, **257**, 414.
- (a) M. Girhard and V. B. Urlacher, *Modern Oxidation Methods*, Wiley-VCH Verlag GmbH & Co. KGaA, 2010, p. 421; (b) J. T. Groves, *J. Inorg. Biochem.*, 2006, **100**, 434; (c) D. Hamdane, H. Zhang and P. Hollenberg, *Photosynth. Res.*, 2008, **98**, 657; (d) P. R. Ortiz de Montellano, *Chem. Rev.*, 2010, **110**, 932; (e) V. B. Urlacher and M. Girhard, *Trends Biotechnol.*, 2012, **30**, 26.
- (a) A. N. Biswas, M. Puri, K. K. Meier, W. N. Oloo, G. T. Rohde, E. L. Bominaar, E. Münck and L. Que, Jr., *J. Am. Chem. Soc.*, 2015, **137**, 2428; (b) M. Ghosh, K. K. Singh, C. Panda, A. Weitz, M. P. Hendrich, T. J. Collins, B. B. Dhar and S. Sen Gupta, *J. Am. Chem. Soc.*, 2014, **136**, 9524; (c) K. K. Singh, M. K. Tiwari, M. Ghosh, C. Panda, A. Weitz, M. P. Hendrich, B. B. Dhar, K. Vanka and S. Sen Gupta, *Inorg. Chem.*, 2015, **54**, 1535; (d) P. Barman, A. K. Vardhaman, B. Martin, S. J. Wörner, C. V. Sastri and P. Comba, *Angew. Chem., Int. Ed.*, 2015, **54**, 2095; (e) T. A. Jackson, J.-U. Rohde, M. S. Seo, C. V. Sastri, R. DeHont, A. Stubna, T. Ohta, T. Kitagawa, E. Münck, W. Nam and L. Que, Jr., *J. Am. Chem. Soc.*, 2008, **130**, 12394; (f) K. Ray, J. England, A. T. Fiedler, M. Martinho, E. Münck and L. Que, Jr., *Angew. Chem., Int. Ed.*, 2008, **47**, 8068; (g) S. A. Wilson, J. Chen, S. Hong, Y.-M. Lee, M. Clémancey, R. Garcia-Serres, T. Nomura, T. Ogura, J.-M. Latour, B. Hedman, K. O. Hodgson, W. Nam and E. I. Solomon, *J. Am. Chem. Soc.*, 2012, **134**, 11791; (h) A. R. McDonald, Y. Guo, V. V. Vu, E. L. Bominaar, E. Münck and L. Que, Jr., *Chem. Sci.*, 2012, **3**, 1680; (i) F. T. de Oliveira, A. Chanda, D. Banerjee, X. Shan, S. Mondal, L. Que Jr., E. L. Bominaar, E. Münck and T. J. Collins, *Science*, 2007, **315**, 835; (j) S. Kundu, J. V. K. Thompson, A. D. Ryabov and T. J. Collins, *J. Am. Chem. Soc.*, 2011, **133**, 18546.
- (a) J. Kaizer, E. J. Klinker, N. Y. Oh, J.-U. Rohde, W. J. Song, A. Stubna, J. Kim, E. Münck, W. Nam and L. Que, Jr., *J. Am. Chem. Soc.*, 2003, **126**, 472; (b) C. V. Sastri, S. M. Sook, P. M. Joo, K. K. Mook and W. Nam, *Chem. Commun.*, 2005, 1405; (c) H. Hirao, D. Kumar, L. Que, Jr. and S. Shaik, *J. Am. Chem. Soc.*, 2006, **128**, 8590; (d) D. Kumar, S. P. de Visser and S. Shaik, *J. Am. Chem. Soc.*, 2003, **125**, 13024; (e) D. Kumar, H. Hirao, L. Que, Jr. and S. Shaik, *J. Am. Chem. Soc.*, 2005, **127**, 8026; (f) D. Kumar, B. Karamzadeh, G. N. Sastri and S. P. de Visser, *J. Am. Chem. Soc.*, 2010, **132**, 7656; (g) W. Nam, *Acc. Chem. Res.*, 2007, **40**, 522; (h) W. Nam, Y.-M. Lee and S. Fukuzumi, *Acc. Chem. Res.*, 2014, **47**, 1146; (i) S. Ye and F. Neese, *Proc. Natl. Acad. Sci. U. S. A.*, 2011, **108**, 1228; (j) Y. J. Jeong, Y. Kang, A.-R. Han, Y.-M. Lee, H. Kotani, S. Fukuzumi and W. Nam, *Angew. Chem., Int. Ed.*, 2008, **47**, 7321; (k) W. Lai, C. Li, H. Chen and S. Shaik, *Angew. Chem., Int. Ed.*, 2012, **51**, 5556; (l) C. Geng, S. Ye and F. Neese, *Angew. Chem., Int. Ed.*, 2010, **49**, 5717; (m) P. Comba, M. Maurer and P. Vadivelu, *Inorg. Chem.*, 2009, **48**, 10389.
- K.-B. Cho, X. Wu, Y.-M. Lee, Y. H. Kwon, S. Shaik and W. Nam, *J. Am. Chem. Soc.*, 2012, **134**, 20222.
- (a) X. Wu, M. S. Seo, K. M. Davis, Y.-M. Lee, J. Chen, K.-B. Cho, Y. N. Pushkar and W. Nam, *J. Am. Chem. Soc.*, 2011, **133**, 20088; (b) E. Kwon, K.-B. Cho, S. Hong and W. Nam, *Chem. Commun.*, 2014, **50**, 5572.
- T. Kojima, K. Nakayama, K. Ikemura, T. Ogura and S. Fukuzumi, *J. Am. Chem. Soc.*, 2011, **133**, 11692.
- See ESI†.
- M. Lubben, A. Meetsma, E. C. Wilkinson, B. L. Feringa and L. Que Jr., *Angew. Chem., Int. Ed.*, 1995, **34**, 1512.
- E. J. Klinker, J. Kaizer, W. W. Brennessel, N. L. Woodrum, C. J. Cramer and L. Que Jr., *Angew. Chem., Int. Ed.*, 2005, **44**, 3690.
- G. Roelfes, M. Lubben, K. Chen, R. Y. N. Ho, A. Meetsma, S. Genseberger, R. M. Hermant, R. Hage, S. K. Mandal, V. G. Young, Y. Zang, H. Kooijman, A. L. Spek, L. Que Jr and B. L. Feringa, *Inorg. Chem.*, 1999, **38**, 1929.
- (a) G. Roelfes, V. Vrajmasu, K. Chen, R. Y. N. Ho, J.-U. Rohde, C. Zondervan, R. M. la Crois, E. P. Schudde, M. Lutz, A. L. Spek, R. Hage, B. L. Feringa, E. Münck and L. J. Que Jr., *Inorg. Chem.*, 2003, **42**, 2639; (b) D. Wang, K. Ray, M. J. Collins, E. R. Farquhar, J. R. Frisch, L. Gomez, T. A. Jackson, M. Kerscher, A. Waleska, P. Comba, M. Costas and L. Que, Jr., *Chem. Sci.*, 2013, **4**, 282; (c) M. J. Collins, K. Ray and L. J. Que Jr., *Inorg. Chem.*, 2006, **45**, 8009.
- (a) A. Decker, J.-U. Rohde, E. J. Klinker, S. D. Wong, L. Que Jr and E. I. Solomon, *J. Am. Chem. Soc.*, 2007, **129**, 15983; (b) A. Decker, J.-U. Rohde, L. Que Jr and E. I. Solomon, *J. Am. Chem. Soc.*, 2004, **126**, 5378.
- M. S. Seo, J.-H. In, S. O. Kim, N. Y. Oh, J. Hong, J. Kim, L. Que Jr and W. Nam, *Angew. Chem., Int. Ed.*, 2004, **43**, 2417.
- J. J. Braymer, K. P. O'Neill, J.-U. Rohde and M. H. Lim, *Angew. Chem., Int. Ed.*, 2012, **51**, 5376.
- N. Y. Oh, Y. Suh, M. J. Park, M. S. Seo, J. Kim and W. Nam, *Angew. Chem., Int. Ed.*, 2005, **44**, 4235.
- S. Kumar, A. S. Faponle, P. Barman, A. K. Vardhaman, C. V. Sastri, D. Kumar and S. P. de Visser, *J. Am. Chem. Soc.*, 2014, **136**, 17102.
- (a) Y. Nishida, Y. Morimoto, Y.-M. Lee, W. Nam and S. Fukuzumi, *Inorg. Chem.*, 2013, **52**, 3094; (b) A. Draksharapu, D. Angelone, M. G. Quesne, S. K. Padamati, L. Gómez, R. Hage, M. Costas, W. R. Browne and S. P. de Visser, *Angew. Chem., Int. Ed.*, 2015, **54**, 4357–4361; (c) J. Yoon, S. A. Wilson, Y. K. Jang, M. S. Seo, K. Nehru, B. Hedman, K. O. Hodgson, E. Bill, E. I. Solomon and W. Nam, *Angew. Chem., Int. Ed.*, 2009, **48**, 1257; (d) S. Rana, S. Bag, T. Patra and D. Maiti, *Adv. Synth. Catal.*, 2014, **356**, 2453.
- J. R. Bryant and J. M. Mayer, *J. Am. Chem. Soc.*, 2003, **125**, 10351.
- (a) T. Kojima, R. A. Leising, S. Yan and L. Que Jr., *J. Am. Chem. Soc.*, 1993, **115**, 11328; (b) L. Mathew and J. Warkentin, *Can. J. Chem.*, 1988, **66**, 11; (c) J. T. Groves and T. E. Nemo, *J. Am. Chem. Soc.*, 1983, **105**, 6243.
- A. A. Fokin and P. R. Schreiner, *Chem. Rev.*, 2002, **102**, 1551.

